An Integrated Passive Islanding Detection Method for Distributed Generators

WEN-YEAU CHANG
Department of Electrical Engineering
St. John's University
HONG-TZER YANG *
* Department of Electrical Engineering
* National Cheng Kung University
No. 499, Sec. 4, Tam King Road, Tamsui, Taipei 251, Taiwan
* No. 1, University Road, Tainan City 701, Taiwan
TAIWAN
changwy@mail.sju.edu.tw
* htyang@mail.ncku.edu.tw

Abstract: - This study proposes a new islanding detection method for use of grid-interconnected distributed generators (DG). The method is based on two indices: the rate of change of frequency (ROCOF) and the rate of change of voltage (ROCOV). When a DG is grid-interconnected, the ROCOF and ROCOV are lower than the threshold value. In contrast, as an islanding occurs, the ROCOF or ROCOV become much higher than the threshold values. Detection systems monitor terminal voltage at the grid-interconnected point to calculate ROCOF and ROCOV, and issue an operating signal when the value and duration of ROCOF or ROCOV exceed a given threshold. In this study, experiments are conducted to illustrate the principles of the proposed technique for both synchronous generators and induction generators. The test results show that the newly proposed method is reliable, economical, and easy to implement for islanding detection of distributed generators.

Key-Words: - Islanding detection, Distributed generator, Rate of change of frequency, Rate of change of voltage

1 Introduction

Rising crude oil prices and worldwide awareness of environmental issues are leading to the exploitation of distributed generation systems. A distributed generation system is defined as the power generation system inside the distribution system. To generate electricity, distributed generation systems are driven by prime movers such as wind turbines, water turbines, micro-turbines, etc. Due to technological innovations related to energy conversion in the last decade, the competitive generation of electricity is now possible with distributed generation units.

Many previous studies have explored the sizing, placement, reliability, and expansion planning of distributed generation systems [1-6]. The main merits of distributed generation systems can be listed as follows: reduction of power loss, voltage profile improvement, power quality improvement, the possibility to exploit combined heat and power generation, simple structure, high efficiency, and minimal environmental impact. Since distributed generation systems are inside distribution system, they change the characteristics of the distribution systems, thus, affecting voltage regulation and protection schemes [7-10].

An essential requirement of a grid-interconnected distributed generation system is islanding detection capability [11]. Islanding occurs when a part of the distribution system is electrically isolated from the main source of supply, yet continues to be energized by the DG. The islanding operation of a DG may cause potential hazards to line-maintenance personnel, and risk damage of the DG by out-of phase reconnection to the grid. The majority of utilities require that DG should be disconnected from the grid as soon as islanding occurs. IEEE standard 1547 stipulates a maximum delay of 2 seconds for detection of an islanding [12].

Islanding detection methods can be generally categorized into two groups, passive methods and active methods. Passive methods detect islanding operation of DGs by monitoring selected power system parameters, such as voltage magnitude, change rate of frequency, phase displacement, and power output. The passive methods include the change of voltage magnitude relay [13], the rate of change of frequency relay [14], the vector surge relay [15], the voltage unbalance and total harmonic distortion of current relay [16], the change of output power relay [17], the ratio of the frequency change to the output power change relay [18], the rate of change of voltage and power factors relay [19], as well as the logical rule-based detection technique [20]. The principles of these methods were developed based on the fact that an islanding causes variations system parameters.

However, when the amount of the power mismatch between a DG and a local load is not significant enough during islanding, the methods mentioned above may fail to signal the abnormality. Furthermore, another drawback to passive methods is that they cannot effectively differentiate between islanding and other non-islanding transients, like voltage flicker or sag.

The four main active islanding detection methods are the reactive error export detection method, the positive feedback for power loop method, the voltage fluctuation correlated method, and the correlation factor method.

The reactive error export detection method controls the excitation current of distributed generation systems so that they generate a known value of reactive current, which cannot be supported unless the generator is connected to the grid [21].

The positive feedback for power loop method results in an unstable frequency or voltage, once the distributed generation system is islanded. Eventually, the unstable frequency or voltage will trip the frequency or voltage relay to protect islanding [22]. Small-scale distributed generation systems have simple excitation, sometimes using permanent magnets. Hence, islanding of small-scale distributed generation system cannot be detected effectively by controlling reactive power export, as in the reactive error export detection method or the positive feedback for power loop method.

The voltage fluctuation correlated method uses power transistors to switch high-impedance loads periodically near the voltage zero crossing point. This method measures the voltage fluctuation through the utility-interconnected point, enabling evaluation of the source impedance of system and detection of islanding. It provides a very effective means of detection, with the disadvantage of introducing a small voltage perturbation at the zero crossing point [23].

The correlation factor method for DGs is based on voltage fluctuation injection, which can be obtained through high-impedance load switching on the grid periodically [24-25], or regulating the field current of the distributed synchronous generator periodically [26]. The correlation factor between the periodic trigging signal and the perturbed voltage is then used as an islanding detection index in the proposed islanding detection method. When a DG is grid-interconnected, the correlation factor is lower than the threshold value. In contrast, as an islanding occurs, the correlation factor becomes much higher than the threshold value.

Active methods are more effective and robust than passive ones, but most existing active schemes have the disadvantages of high cost and a certain degree of degradation of power quality.

To overcome the disadvantages of the existing islanding detection methods, the aim of this study is to propose a new integrated passive islanding detection method for grid-interconnected DGs. As described below, the proposed method is more effective and economical than the conventional islanding detection methods.

This study is organized as follows. The basic principle of the ROCOF detection method is described in section 2. The principle of the ROCOV detection method is described in section 3. The principles of the proposed integrated detection system are given subsequently. The experimental results and the analysis using a distributed synchronous generator and distributed induction generator are presented in section 5. The test results demonstrate the effectiveness of the proposed method to improve the detection accuracy. The conclusions of this study are given in the last section.

2 Basic Principle of the ROCOF Detection Method

The ROCOF detection method is based on the feature that the real power imbalance causes transients in an islanded systems and the system frequency starts to vary dynamically during the islanding operation. Such system behavior can be used to detect an islanding condition. Therefore, measuring the ROCOF would show whether the DG is operating in parallel with the grid or functioning independently of the grid.

The equivalent circuit of a DG interconnected to the grid in normal operation is shown in Fig. 1, where P_L is the local load demand; P_g is the active power generation of the DG; P_u is the active power supplied by the power grid. The active power balance equation when the DG is interconnected to the grid is expressed as:

$$P_u + P_g = P_L \tag{1}$$

The equivalent circuit of a DG subject to islanding operation is shown in Fig. 2. After opening of the tie switch S_1, the DG starts running in an islanded mode and a power imbalance exists due to the lost grid power P_u. Such active power imbalance ΔP is described as follows:

$$\Delta P = P_g - P_L = -P_u \tag{2}$$

The swing equation of the DG during islanding operation is given by

$$\frac{2H}{\omega_0} \times \frac{d\omega}{dt} = \Delta P = P_g - P_L \tag{3}$$

where H is the inertia constant of the DG, ω is the rotor speed of the DG, ω_0 is the synchronous speed in normal operation. The derivative of ω can be solved from (3) as:

$$\frac{d\omega}{dt} = \frac{\omega_0 \Delta P}{2H} \tag{4}$$

Since ω and ω_0 can be described as $\omega = 2\pi f$ and $\omega_0 = 2\pi f_0$, where f is the system frequency in an islanding operation, f_0 is the system synchronous frequency in normal operation. The ROCOF ($\Delta f/\Delta t$) can be solved from (4) as:

$$\frac{\Delta f}{\Delta t} = \frac{df}{dt} = \frac{f_0 \Delta P}{2H} \tag{5}$$

As shown in (5), when the real power imbalance ΔP causes transients in the islanded system, the frequency of the system drifts up or down, making the frequency of the system deviate from its nominal value until frequency relay is triggered. However, if the power imbalance ΔP in the islanded system is small, then the frequency will change slowly. Thus, ROCOF can be used as a detection index under this islanding situation [14].

3 Basic Principle of the ROCOV Detection Method

The ROCOV detection method is based on the feature that the reactive power imbalance causes transients in an islanded system and the terminal voltage starts to vary dynamically during the islanding operation. As in the principle of the ROCOF mentioned above, such system behavior can also be used to detect an islanding condition. Therefore, measuring the ROCOV would show whether the DG is operating in parallel with the grid or functioning independently of the grid.

As shown in Fig. 1, we have the equivalent circuit of a DG parallel with the grid in normal operation, where $E_u = |E_u|\angle\delta_u$ and $E_g = |E_g|\angle\delta_g$ are the open circuit voltages of the utility and the DG;

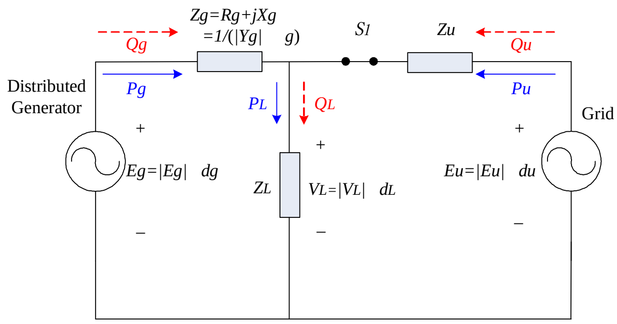

Fig. 1 Equivalent circuits of a DG parallel with the grid

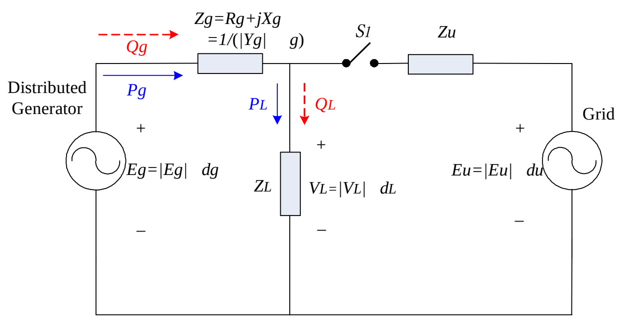

Fig. 2 Equivalent circuits of a DG during islanding operation

$V_L = |V_L|\angle\delta_L$ is the terminal voltage of the local load; Z_u is the source impedance of the utility grid; $Z_g = R_g + jX_g = 1/(|Y_g|\angle\theta_g)$ is the source impedance of the DG; Z_L is the local load impedance; Q_L is the local reactive load demand; Q_g is the reactive power generation of the DG; Q_u is the reactive power provided by the power grid. The reactive power balance equation when the DG is interconnected to the grid is expressed as:

$$Q_u + Q_g = Q_L \tag{6}$$

As shown in Fig. 2, after opening the tie switch S_1, the DG starts running in an islanded mode and a reactive power imbalance exists due to the lost grid reactive power Q_u. Such reactive power imbalance ΔQ is described as follows:

$$\Delta Q = Q_g - Q_L = -Q_u \tag{7}$$

The reactive power generation of DG is given by

$$Q_g = -|E_g||V_L||Y_g|\sin(\theta_g - \delta_g + \delta_L) \tag{8}$$

The partial derivative of Q_g can be solved from (8) as:

$$\frac{\partial Q_g}{\partial |V_L|} = -|E_g||Y_g|\sin(\theta_g - \delta_g + \delta_L) \tag{9}$$

Since $\theta_g - \delta_g + \delta_L \cong \theta_g$, (9) can be approximately expressed as:

$$\frac{\partial Q_g}{\partial |V_L|} \cong -|E_g||Y_g|\sin(\theta_g) = -|E_g|B_g \qquad (10)$$

where B_g is the imaginary part of Y_g. Eq. (10) can be solved as:

$$\frac{\Delta Q_g}{|E_g|} \cong -B_g \Delta |V_L| \qquad (11)$$

Because $\Delta Q_g = -\Delta Q$, (11) can be written as:

$$\Delta |V_L| \cong \frac{1}{B_g} \times \frac{\Delta Q}{|E_g|} \qquad (12)$$

If the armature resister of the DG (R_g) is ignored, B_g can be approximately expressed as $1/X_g$, where X_g is the source reactance of the DG. Then, ROCOV ($\Delta|V_L|/\Delta t$) can be solved as:

$$\frac{\Delta |V_L|}{\Delta t} \cong \frac{X_g}{|E_g|} \times \frac{\Delta Q}{\Delta t} \qquad (13)$$

As shown in (13), when the reactive power imbalance ΔQ causes transients in the islanded system, the terminal voltage drifts up or down, making the terminal voltage deviate from its nominal value until voltage relay is triggered. However, if the reactive power imbalance ΔQ in the islanded system is small, then the terminal voltage will change slowly, due to small value of ROCOV. Thus, ROCOV can be used as an alternative detection index in this kind of islanding situation.

4 The Proposed Integrated Detection System

The architecture of the proposed integrated islanding detection system is illustrated in Fig. 3. A voltage detecting interface measures the magnitude of terminal voltage at the grid-interconnected point; and a zero crossing detecting circuit detects the zero crossing signal of the terminal voltage. A digital signal processor (DSP) calculates the ROCOF and ROCOV of the terminal voltage and decides whether the trip conditions are met.

Fig. 4 depicts the proposed procedure of the integrated detection method. It consists of terminal voltage detection, zero crossing detection, ROCOF calculation, ROCOV calculation, and decision process. The procedure is built up in a DSP program using C language. As shown in Fig. 4, the decision process of the program has 4 threshold values as the

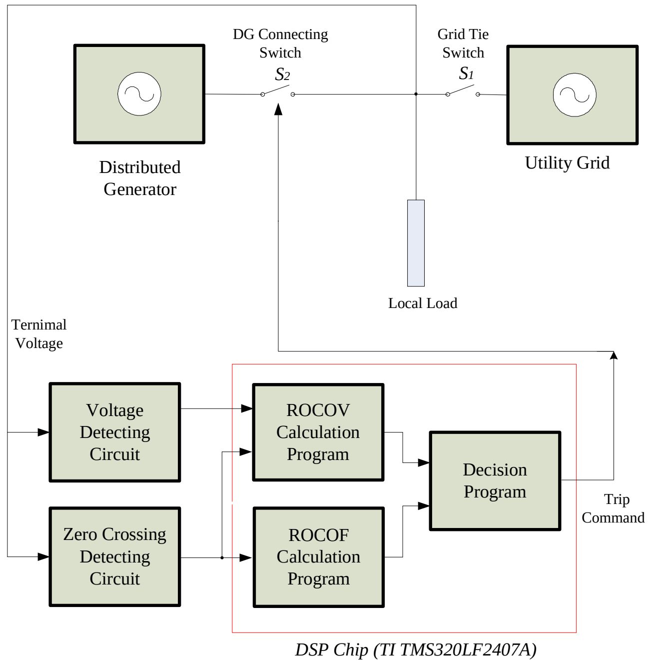

Fig. 3 System configuration of the integrated islanding detector

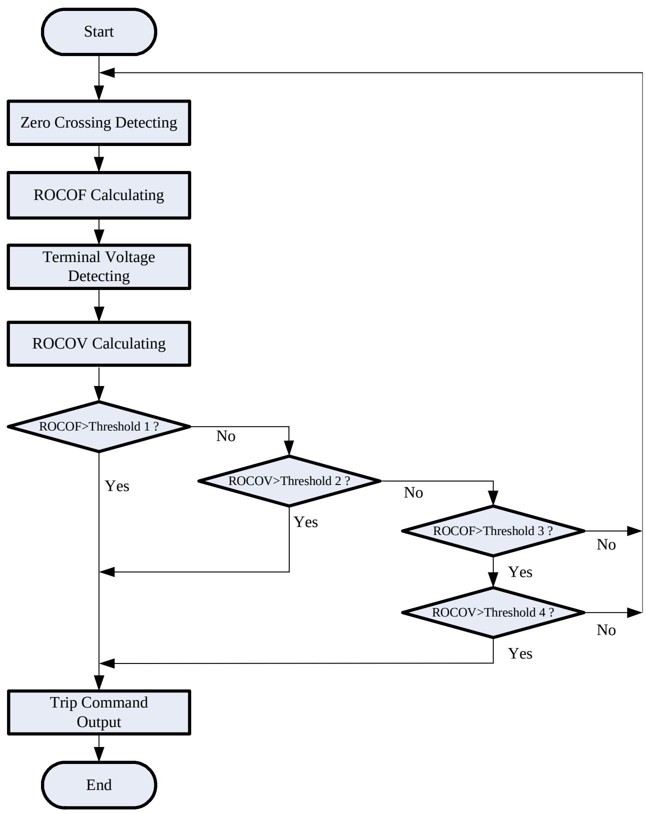

Fig. 4 Proposed procedure of the integrated islanding detection method

islanding detection indices. For larger real power imbalance ΔP, the index of ROCOF (Threshold 1) is set as 0.5 Hz/s in this study. Similarly, for larger reactive power imbalance ΔQ, the index of ROCOV (Threshold 2) is set as 4 V/s. Moreover, for the smaller real and reactive power imbalances occurring simultaneously, the indices of ROCOF and ROCOV (Threshold 3 and Threshold 4) are set as 0.12 Hz/s and 2 V/s respectively.

5 Experimental Results

To verify the proposed method, experiments were conducted to demonstrate its effectiveness as an islanding detection approach. The experimental tests were carried out on two kinds of generators: synchronous generators and induction generators. The procedures of the tests were to verify that the DG systems cease to energize the utility grid when an unintentional island condition is present.

5.1 Islanding test for synchronous generators

A prototypical islanding detector for synchronous generators was set up in the laboratory. The distributed synchronous generator employed in the tests consisted of a grid-interconnected, three-phase, 220V, 300W synchronous generator driven by a DC motor with 4 types of loads, including light resistive load, heavy resistive load, inductive and capacitive ones. The test circuit was configured as shown in Fig. 5. The distributed synchronous generator was started, synchronized to the utility grid, and then the tie-switch S_2 was closed to interconnect the distributed synchronous generator to the grid. Open switch S_1 and record the time between the opening of switch S_1 and when the distributed synchronous generator ceases to energize the load. The test is successful when the distributed synchronous generator ceases to energize the test load within the timing requirements of IEEE Standard 1547 after switch S_1 is opened.

The experiments that randomly switched the loads verified the capability of the proposed system to avoid false alarm. The random load switching tests were conducted 200 times for each kind of load. The results depict that no false alarm occurred during the 800 switching tests. As an example of typical test of random load switching, Fig. 6 shows that the detection system did not have false alarm due to a typical load switching. In Fig. 6, Channel 1 denotes the waveform of grid voltage, Channel 2 indicates the waveform of local load terminal voltage, Channel 3 depicts the waveform of load current, and Channel 4 shows the tripping signal. The amplification ratio of the isolated voltage probe for Channel 1 and 2 was

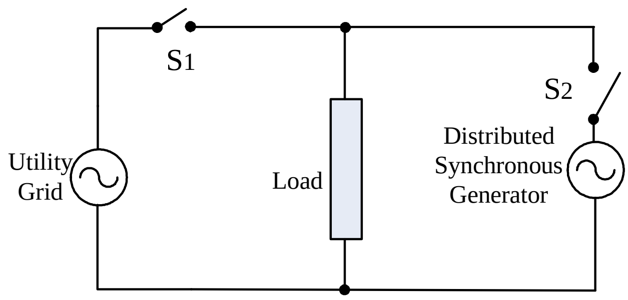

Fig.5 The islanding test configuration for synchronous generators

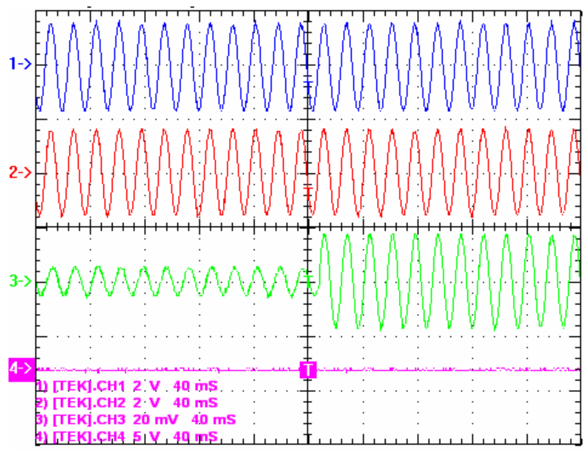

CH1:400V/div, CH2:400V/div, CH3:2A/div, CH4:5V/div, Time:40ms/div

Fig. 6 Results of the experiment for synchronous generator that randomly switched the load

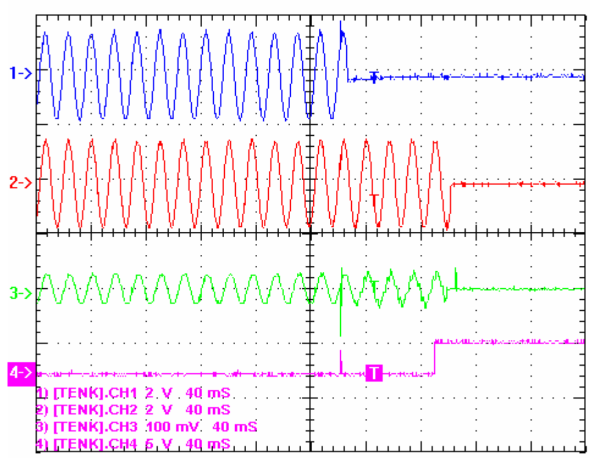

CH1:400V/div, CH2:400V/div, CH3:1A/div, CH4:5V/div, Time:40ms/div

Fig. 7 Results of the experiment for synchronous generator using light resistive load set to be 200 and the transfer ratio of the current probe for Channel 3 was set to be 10mV/A.

To further verify the proposed detection system, the islanding detection tests were conducted for four kinds of loads at random time points, including (a) light resistive loads, (b) heavy resistive loads, (c) inductive loads, (d) capacitive loads. Islanding was successfully detected by all the tests. An example of a typical test for light resistive loads is shown in Fig. 7. In the experiments, the resistance of the resistive load used was 767Ω. The islanding detection signal was issued in 0.075 seconds (a total of 4.5 cycles were needed to estimate the differential voltage magnitudes) after the islanding operation. In a typical test for heavy resistive loads, resistance of the load used was 256Ω. As illustrated in Fig. 8, the islanding detection signal of islanding was given in 0.075 seconds (a total of 4.5 cycles needed) after the islanding operation. In the typical test for inductive loads, we used a load of 256Ω resistance, 444mH inductance, and 17.87μF capacitance. Fig. 9 shows that the islanding detection signal was given in 0.10 seconds (a total of 6 cycles needed) after the islanding operation. In the typical test for capacitive loads, this study used a load of 256Ω resistance, 296mH inductance, and 17.87μF capacitance. As shown in Fig. 10, the islanding detection signal was likewise announced successfully in 0.125 seconds (a total of 7.5 cycles needed) after the islanding operation. In Fig. 7 to Fig. 10, Channel 1 denotes the waveform of grid voltage, Channel 2 indicates the waveform of local load terminal voltage, Channel 3 depicts the waveform of load current, and Channel 4 shows the tripping signal. The amplification ratio of the isolated voltage probe for Channel 1 and 2 was set to be 200 and the transfer ratio of the current probe for Channel 3 was set as 100A/mV.

The effectiveness of the proposed method has been validated in the experiments for synchronous generators. The testing results show that the ROCOF and ROCOV used as the indices of islanding detection, can detect islanding operation easily and accurately. The verification results also reveal that the proposed integrated method detected the islanding event with a maximum delay time of 0.125 seconds for the four kinds of loads used in this study. The detection time needed is much less than the maximal 2 seconds as specified by IEEE standard 1547.

5.2 Islanding test for induction generators

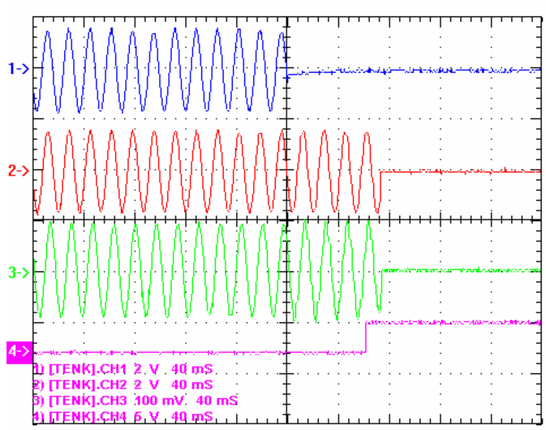

CH1:400V/div, CH2:400V/div, CH3:1A/div, CH4:5V/div, Time:40ms/div

Fig. 8 Results of the experiment for synchronous generator using heavy resistive load

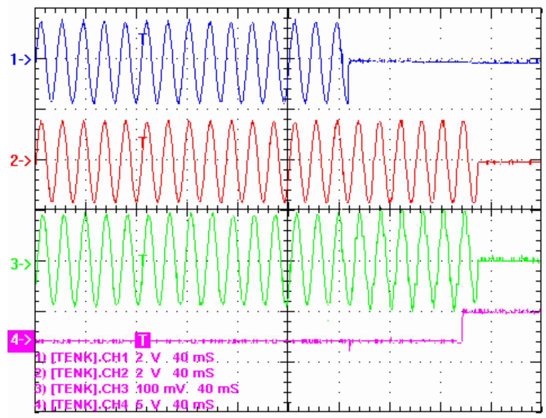

CH1:400V/div, CH2:400V/div, CH3:1A/div, CH4:5V/div, Time:40ms/div

Fig. 9 Results of the experiment for synchronous generator using inductive load

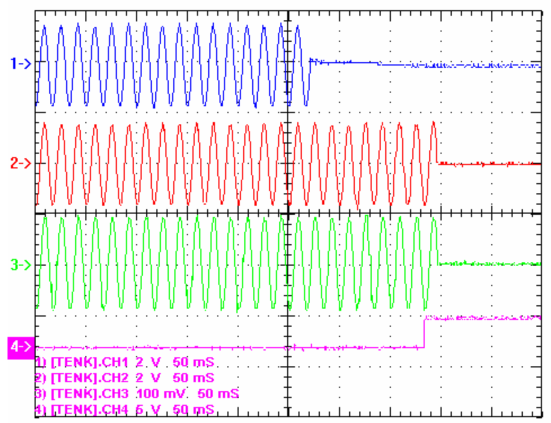

CH1:400V/div, CH2:400V/div, CH3:1A/div, CH4:5V/div, Time:50ms/div

Fig. 10 Results of the experiment for synchronous generator using capacitive load

The generation system employed in the islanding tests for induction generators consisted of a grid-interconnected, three-phase, 220V, 300W induction generator driven by a DC motor with 5 types of loads, including (a) a 50% rated load at unity power factor, (b) a 60% rated load at unity power factor, (c) a 90% rated load at unity power factor, (d) a 100% rated load at unity power factor, (e) a 120% rated load at unity power factor. The test circuit was configured as shown in Fig. 11. The distributed induction generator was started, synchronized to the utility grid, and then the tie-switch S_2 was closed to interconnect the distributed induction generator to the utility grid. We adjusted the islanding RLC load circuit, as shown in Fig. 11 to provide a quality factor of 1.0 ± 0.05. The reactive load was balanced so that the resonant frequency of the island circuit was within the under-frequency (59.5Hz) and over-frequency (60.5Hz) trip settings of the distributed induction generator and as close to nominal frequency (60Hz) as possible. Upon opening of switch S_1, time was recorded between the opening of switch S_1 and the time when the distributed induction generator ceased to energize the load. The test was successful when the distributed induction generator ceased to energize the test load within the timing requirements of IEEE Standard 1547 after switch S_1 is opened.

The experiments that randomly switched the loads verified the capability of the proposed system to avoid false alarm. The random load switching tests were conducted 200 times for each kind of load. The results depict that no false alarm occurred during of the 1000 switching tests. As an example of a typical test for random load switching, Fig. 12 exhibits that the detection system did not have a false alarm due to the load switching. In Fig. 12, Channel 1 denotes the waveform of grid voltage, Channel 2 indicates the waveform of local load terminal voltage, Channel 3 depicts the waveform of load current, and Channel 4 shows the tripping signal. The amplification ratio of the isolated voltage probe for Channel 1 and 2 was set to be 200 and the transfer ratio of the current probe for Channel 3 was set to be 100 mV/A.

In a typical test using the type (a) load, as shown in Fig. 13, the islanding detection signal was issued in 0.092 seconds (a total of 5.5 cycles were needed to estimate the differential voltage magnitudes) after the islanding operation started.

In the typical test using a type (b) load, as shown in Fig. 14, the islanding detection signal was likewise announced successfully in 0.067 seconds (a total of 4 cycles needed) after the islanding operation started.

In the typical test using a type (c) load, as shown in Fig. 15, the islanding detection signal was likewise announced successfully in 0.042 seconds (a total of

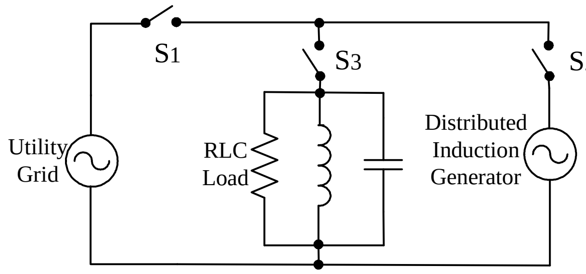

Fig.11 The islanding test configuration for induction generators

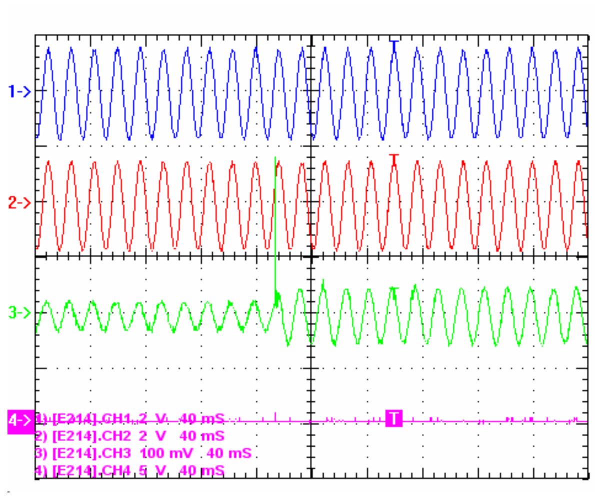

CH1:400V/div, CH2:400V/div, CH3:1A/div, CH4:5V/div, Time:40ms/div

Fig. 12 Results of the experiment for induction generator in case of random switching of the load

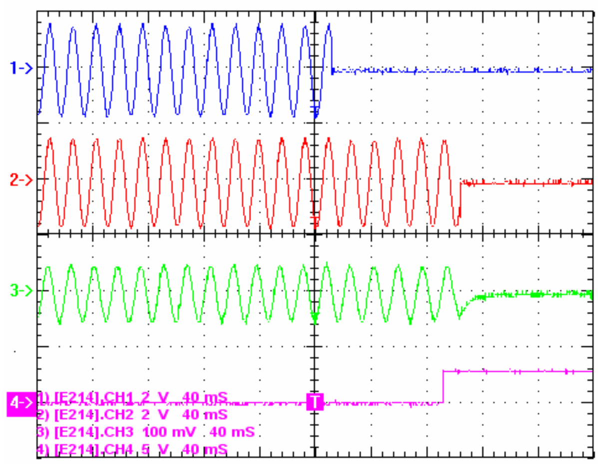

CH1:400V/div, CH2:400V/div, CH3:1A/div, CH4:5V/div, Time:40ms/div

Fig. 13 Results of the experiment for induction generator using a type (a) load

2.5 cycles needed) after the islanding operation started.

In the typical test using a type (d) load, as shown in Fig. 16, the islanding detection signal was likewise announced successfully in 0.083 seconds (a total of 5 cycles needed) after the islanding operation started.

In the typical test using a type (e) load, as shown in Fig. 17, the islanding detection signal was likewise announced successfully in 0.042 seconds (a total of 2.5 cycles needed) after the islanding operation started.

In Figs. 13 to 17, Channel 1 denotes the waveform of grid voltage, Channel 2 indicates the waveform of local load terminal voltage, Channel 3 depicts the waveform of load current and Channel 4 shows the tripping signal. The amplification ratio of the isolated voltage probe for Channel 1 and 2 was set to be 200 and the transfer ratio of the current probe for Channel 3 was set as 100mV/A.

The effectiveness of the proposed method has been validated in the experiments for synchronous generators. The testing results show that the ROCOF and ROCOV used as the indices of islanding detection, can detect islanding operation easily and accurately. The verification results also reveal that the proposed integrated method detected the islanding event with a maximum delay time of 0.092 seconds for the three kinds of loads used in this study. The detection time needed is much less than the maximal 2 seconds as specified by IEEE standard 1547.

6 Conclusions

Based on an integrated detection scheme, this study has proposed a new method to quickly and reliably detect the islanding operation of a DG system. The indices of ROCOF and ROCOV of the terminal voltage are calculated by a DSP. Observing the ROCOF and ROCOV of the proposed scheme through the DSP system, discrimination between islanding and other non-islanding disturbances can thus be made accurately.

To verify the effectiveness of the proposed technique, experiments using different kinds of typical loads were used in this study. The experiment results show that the proposed indices of the islanding detection of ROCOF and ROCOV can detect the islanding operations satisfactorily for the different kinds of loads within 0.125 seconds. The detection performance is verified to be less dependent on the load quality factor and power level.

The directions of future research of the islanding detection methods can be described as follows: To further improve the detection performance of the

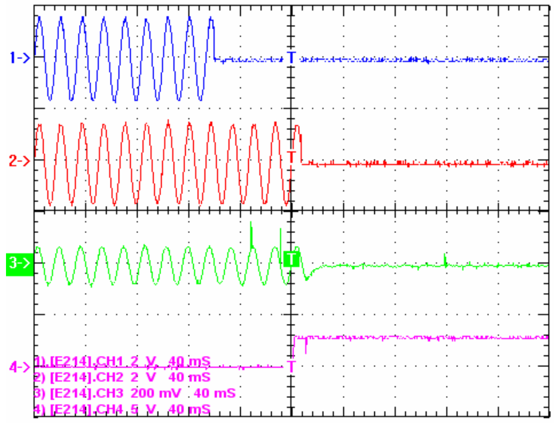

CH1:400V/div, CH2:400V/div, CH3:2A/div, CH4:5V/div, Time:40ms/div

Fig. 14 Results of the experiment for induction generator using a type (b) load

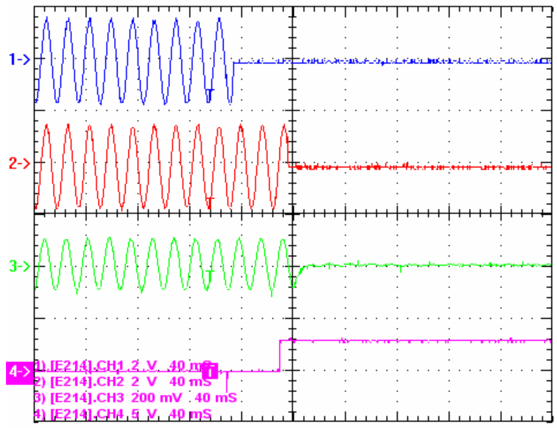

CH1:400V/div, CH2:400V/div, CH3:2A/div, CH4:5V/div, Time:40ms/div

Fig. 15 Results of the experiment for induction generator using a type (c) load

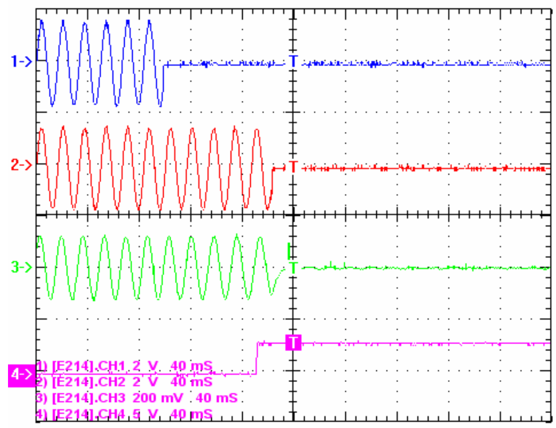

CH1:400V/div, CH2:400V/div, CH3:2A/div, CH4:5V/div, Time:40ms/div

Fig. 16 Results of the experiment for induction generator using a type (d) load

d

proposed passive islanding detection method, the active islanding detection method based on voltage fluctuation injection will be investigated and integrated in the proposed passive method.

7 Acknowledgements

The authors would like to express their acknowledgements to the National Science Council of ROC for the financial support under Grant No. NSC 95-2221-E-129-012.

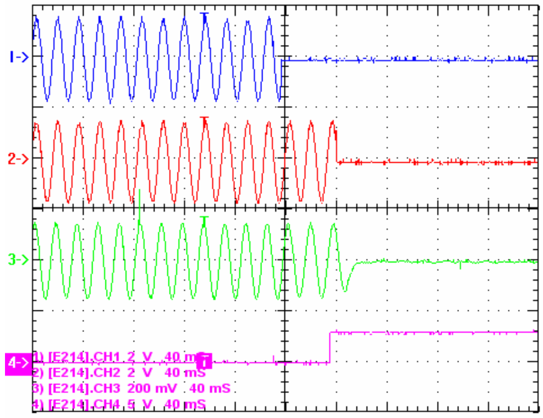

CH1:400V/div,CH2:400V/div,CH3:2A/div,CH4:5V/div, Time:40ms/div

Fig. 17 Results of the experiment for induction generator using a type (e) load

References:

[1] M. Gandomkar, Application of Genetic Algorithm to Distribution Network Expansion Planning with Distributed Generation, *Proceedings of the 8th WSEAS International Conference on Electric Power Systems, High Voltages, Electric Machines*, Venice, Italy, November 21-23, 2008, pp. 15-20.

[2] F. Li and N. Sabiri, Monte Carlo Simulation to Evaluate the Reliability Improvement with DG connected to Distribution Systems, *Proceedings of the 8th WSEAS International Conference on Electric Power Systems, High Voltages, Electric Machines*, Venice, Italy, November 21-23, 2008, pp. 177-182.

[3] M.H. Aliabadi, M. Mardaneh, and B. Behbahani, Siting and Sizing of Distributed Generation Unit Using GA and OPF, *Proceedings of the 2nd WSEAS International Conference on Circuits, Systems, Signal and Telecommunications*, Acapulco, Mexico, 2008, pp. 202-206.

[4] A.H. Mantawy and M. Al-Muhaini, A New Particle-Swarm-Based Algorithm for Distribution System Expansion Planning Including Distributed Generation, *Proceedings of the 2nd IASME/WSEAS International Conference on Energy & Environment*, Portoroz, Slovenia, 2007, pp.236-241.

[5] V.E. Santos, A.G. Martins, and C.H. Antunes, A Multi-Objective Model for Sizing and Placement of Distributed Generation, *WSEAS Transactions on Power Systems*, Volume 1, Issue 7, 2006, pp. 1267-1272.

[6] Y.G. Hegazy and M.A. Mostafa, Reliability Indices of Electrical Distributed Generation Systems, *WSEAS Transactions on Systems*, Volume 4, Issue 10, 2005, pp. 1785-1790.

[7] T.H. Chen, M.S. Wang, and N.C. Yang, Impact of Distributed Generation on Voltage Regulation by ULTC Transformer using Various Existing Methods, *Proceedings of the 7th WSEAS International Conference on Power Systems*, Beijing, China, 2007, pp. 158-163.

[8] A.S. Bretas and R.H. Salim, A New Fault Location Technique for Distribution Feeders with Distributed Generation, *WSEAS Transactions on Power Systems*, Volume 1, Issue 5, 2006, pp. 894-900.

[9] K. Maki, S. Repo, and P. Jarventausta, Protection Coordination to Meet the Requirements of Blinding Problems Caused by Distributed Generation, *WSEAS Transactions on Circuits and Systems*, Volume 4, Issue 7, 2005, pp. 674-683.

[10] D. Ardito, S. Conti, N. Messina, and S. Nicotra, Operating Conflicts in Distribution Networks Protection with Distributed Generation, *WSEAS Transactions on Circuits and Systems*, Volume 4, Issue 9, 2005, pp. 1034-1042.

[11] G. Dalke, et al. Application of Islanding Protection for Industrial and Commercial Generators – An IEEE Industrial Application Society Working Group Report, *Proceedings of the 59th Annual Conference on Protective Relay Engineers*, Texas, USA, 2006, pp. 152-163.

[12] IEEE Standard 1547, Standard for Interconnecting Distributed Resources with Electric Power Systems, 2003.

[13] J.C.M. Vieira, D.S. Correa, W. Freitas and W. Xu, Performance Curves of Voltage Relays for Islanding Detection of Distributed Generators, *IEEE Transactions on Power Systems*, Volume 20, No. 3, 2005, pp. 1660-1662.

[14] C.M. Affonso, W. Freitas, W. Xu and L.C.P. da Silva, Performance of ROCOF Relays for Embedded Generation Applications, *IEE*

Proceedings – Generation Transmission Distribution, Volume 152, No.1, 2005, pp.109-114.

[15] W. Freitas, Z. Huang and W. Xu, A Practical Method for Assessing the Effectiveness of Vector Surge Relays for Distributed Generation Applications, *IEEE Transactions on Power Delivery*, Volume 20, No. 1, 2005, pp. 57–63.

[16] S.I. Jang and K.H. Kim, An Islanding Detection Method for Distributed Generations Using Voltage Unbalance and Total Harmonic Distortion of Current, *IEEE Transactions on Power Delivery*, Volume 19, No.2, 2004, pp. 745–752.

[17] M.A. Redfern, O. Usta, G. Fielding, Protection Against Loss of Utility Grid Supply for a Dispersed Storage and Generation Unit, *IEEE Transactions on Power Delivery*, Volume 8, No.3, 1993, pp. 948–954.

[18] F.S Pai, S.J. Huang, A Detection Algorithm for Islanding-Prevention of Dispersed Consumer-Owned Storage and Generating Units, *IEEE Transactions on Energy Conversion*, Volume 16, No. 4, 2001, pp.346–351.

[19] S.K. Salman, D.J. King, G. Weller, New Loss of Mains Detection Algorithm for Embedded Generation Using Rate of Change of Voltage and Changes in Power Factors, *Proceedings of the 7th IEE International Conference on Developments in Power System Protection*, Amsterdam, Netherlands, 2001, pp. 82–85.

[20] S.I. Jang, K.H. Kim, Development of a Logical Rule-Based Islanding Detection Method for Distributed Resources, *Proceedings of the 2002 IEEE Power Engineering Society Winter Meeting*, New York, USA, 2002, pp. 800-806.

[21] J.W. Warin, Loss of Mains Protection, *Proceedings of the ERA Conference on Circuit Protection for Industrial and Commercial Installations*, Landon, UK, 1990, pp. 4/3/1–12.

[22] P. Du, J.K. Nelson, Z. Ye, Active Anti-Islanding Schemes for Synchronous-Machine-Based Distributed Generators, *IEE Proceedings – Generation Transmission Distribution*, Volume 152, No.5, 2005, pp.597-606.

[23] P.D. Hopewell, N. Jenkins, A.D. Cross, Loss-of-Mains Detection for Small Generators, *IEE Proceedings –Electrical Power Application*, Volume 143, No. 3, 1996, pp.225-230.

[24] W.Y. Chang, H.T. Yang, An Active Islanding Protection Method for Distributed Synchronous Generators, *Proceedings of the 7th IET International Conference on Advances Power System Control, Operation and Management*, Hong Kong, China, 2006, Paper No. APSCOM2006-128.

[25] W.Y. Chang, An Active Islanding Detection Method for Small-Scale Distributed Generators, *WSEAS Transactions on Circuits and Systems*, Volume 7, Issue 6, 2008, pp. 547-557.

[26] W.Y. Chang, A Correlation Factor Based Islanding Detection Method for Distributed Synchronous Generators, *WSEAS Transactions on Systems*, Volume 7, Issue 11, 2008, pp. 1329-1338.